INSTITUTE OF PHYSICS PUBLISHING JOURNAL OF OPTICS A: PURE AND APPLIED OPTICS
J. Opt. A: Pure Appl. Opt. **3** (2001) 114–119 www.iop.org/Journals/oa PII: S1464-4258(01)15157-3

Photorefractive amplifier–converter and coherent oscillator with nonexponential gain

P Jullien[1], P Lompré[1], P Mathey[1], S Odoulov[2] and E Krätzig[3]

[1] Laboratoire de Physique, Matériaux pour l'Optique non linéaire, Université de Bourgogne, BP 47870, 21078 Dijon, France
[2] Institute of Physics, National Academy of Sciences, 03 650, Kiev 22, Ukraine
[3] Fachbereich Physik, Universität Osnabrück, D-49 076 Osnabrück, Germany

E-mail: pjullien@u-bourgogne.fr, odoulov@iop.kiev.ua and eckhard.kraetzig@physik.uni-osnabrueck.de

Received 4 July 2000, in final form 16 November 2000

Abstract
For some parametric interactions with identically zero exponential gain for the signal wave the intensity of the idler wave can grow as a second power of the propagation coordinate. Such an amplification is revealed for the parametric mixing of four copropagating waves in $BaTiO_3$; two of them are ordinarily polarized and the two others are extraordinarily polarized. This mixing is used to build up a coherent oscillator. A reasonable qualitative agreement of the experimental results with the calculated data is demonstrated.

Keywords: Parametric interactions, coherent oscillator, photorefractive mixing, barium titanate

1. Introduction

Coherent light amplification with photorefractive crystals may be a consequence of several frequency-degenerate (or nearly degenerate) processes of nonlinear wave mixing: it appears for two-beam coupling in crystals with diffusion-driven charge transport [1] or transport via circular photovoltaic currents [2]. The parametric mixing [3] of three, four or more beams may also result in signal beam amplification. In all these cases, the refractive index gratings recorded in the crystal couple the signal and the pump waves. This coupling results from the pump wave diffraction on the index gratings such that the signal wave gains an additional intensity.

The different types of nonlinear wave mixing are divided into the two following classes: those that ensure a steady-state exponential gain for the weak signal wave and others with an imaginary gain factor, that provide only a transient gain for the signal wave [3]. If for any process the steady state and the transient gain can be achieved with certain configurations (e.g. for different orientations of the signal wave) there always exist values of parameters for which the exponential gain factor is exactly equal to zero.

A zero gain factor does not mean that the signal wave cannot be amplified at all. It may happen that the amplification is achieved with no exponential but power law growth rate in space. The aim of this paper is to show that some types of nonlinear mixing that do not provide either a real or an imaginary exponential gain factor can be used for light amplification and coherent oscillation.

A special kind of frequency degenerate parametric wave mixing is considered where the signal wave is writing a grating with the pump wave but is not amplified itself. At the same time the idler wave exists and is amplified at the expense of the pump wave. The parametric mixing of superimposed copropagating waves of type *A*:ee–eo in the sample [3] governs this amplification process. This allows the design of an amplifier–converter with an output wave that is (i) phase conjugate, (ii) orthogonally polarized and (iii) considerably amplified with respect to the signal wave.

We call this considered amplifier an amplifier–converter to underline that it is not the signal wave itself but a new generated idler wave that gains intensity and finally greatly surpasses the intensity of the incident signal wave. With the correctly introduced feedback such an amplifier–converter may become a coherent oscillator. The parametric process mentioned above is known to produce conical light-induced scattering of a single extraordinary pump wave in $BaTiO_3$ [4–6] and is thus called anisotropic self-diffraction [7, 8], however, it has not yet been

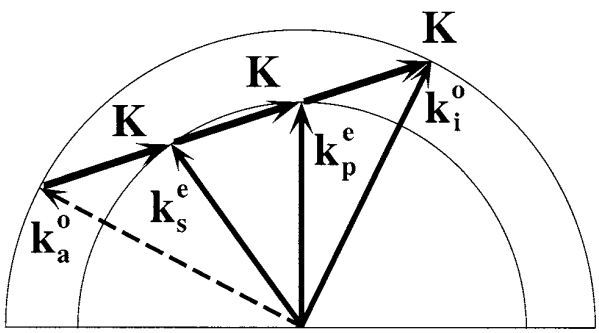

Figure 1. Wavevector diagram of the considered interaction. $\mathbf{k}_p^e$, $\mathbf{k}_s^e$, $\mathbf{k}_i^o$ and $\mathbf{k}_a^o$ are the wavevectors of the pump, signal, idler and additional idler waves respectively, $\mathbf{K}$ is the grating vector.

analysed from the point of view of coherent light amplification.

2. Nonlinear wave mixing

The phase matching diagram is shown in figure 1. The pump wave (with wavevector $\mathbf{k}_p$) is writing an index grating with the signal wave (wavevector $\mathbf{k}_s$); both waves are propagating in the plane normal to the crystal optical axis. The angle between the signal and the pump wave is adjusted in such a way that the phase matching condition is fulfilled:

$$2\mathbf{k}_p^e = \mathbf{k}_s^e + \mathbf{k}_i^o, \tag{1}$$

where $\mathbf{k}_i$ is the wavevector of the idler (i) wave; the superscripts e and o denote, respectively, the extraordinary and ordinary polarization. It follows from equation (1) that the recorded photorefractive grating with the grating vector

$$\mathbf{K} = \mathbf{k}_p^e - \mathbf{k}_s^e = \mathbf{k}_i^o - \mathbf{k}_p^e, \tag{2}$$

couples the pump wave simultaneously to the signal wave and to the idler wave, i.e. parametric mixing of three copropagating waves occurs. For $BaTiO_3$ the pump wave cannot be diffracted from the recorded grating in the direction of the signal wave because of the vanishing electrooptic coefficient r_{331}. At the same time the anisotropic diffraction (with the change of polarization to the orthogonal one) into the idler wave is very efficient because the largest electrooptic coefficient r_{131} is involved.

Let us consider first the experimental geometry with two beams impinging upon the sample, the pump beam with intensity I_p and the signal beam with intensity I_s, both polarized parallel to the crystal C-axis (extraordinary waves). Following the description of the anisotropic diffraction proposed in [8], one can obtain the expression for the output intensity of the idler wave:

$$I_i(\ell) = \frac{I_p(0)}{I_o^2[(\gamma\ell)^2 I_p(0) I_s(0)]^{-1} + 1}, \tag{3}$$

with the coupling constant γ given by

$$\gamma = [8\pi^2 n^3 r_{131} k_B T \sin\theta]/e\lambda^2 \tag{4}$$

where I_o is the total intensity, ℓ is the interaction length, n is the refractive index, k_B is the Boltzmann constant, T is the absolute temperature, λ is the laser wavelength, e is the electron charge and 2θ is the angle between the pump and signal waves in air.

For relatively weak intensities of the signal and idler waves at the output face of the sample in comparison with the pump wave intensity (undepleted pump approximation) equation (3) may be simplified:

$$I_i(\ell) \approx I_s(0)(\gamma\ell)^2 \tag{5}$$

so that the output intensity depends linearly on the signal intensity and increases quadratically with the coupling strength $\gamma\ell$. This last property is distinct from the majority of the other amplification processes in photorefractive crystals with $\pi/2$-shifted index gratings, that lead usually to an exponential growth of the amplified signal with a coupling strength such that $I_s(\ell) \propto \exp(2\gamma\ell)$.

The grating with grating vector $\mathbf{K}$ (equation (2)) also couples the signal wave to an additional idler wave (with wavevector $\mathbf{k}_a$, see figure 1). The calculated coupling strength dependences for the output pump wave, signal wave and additional wave are [8]

$$I_p(\ell) = \frac{I_p(0)}{1 + (\gamma\ell)^2 I_p(0) I_s(0) I_o^{-2}}, \tag{6}$$

$$I_s(\ell) = \frac{I_s(0)}{1 + (\gamma\ell)^2 I_p(0) I_s(0) I_o^{-2}}, \tag{7}$$

$$I_a(\ell) = \frac{I_s(0)}{I_o^2[(\gamma\ell)^2 I_p(0) I_s(0)]^{-1} + 1}. \tag{8}$$

For strong coupling (large $\gamma\ell$) the intensity of the additional wave grows at the expense of the signal wave intensity.

It should be noted that for a pump beam with a plane wavefront the transverse components of the idler wave phase are conjugate to that of the signal wave. This was shown theoretically and proved experimentally in [8], by observing a converging idler wave with a diverging signal wave and vice versa.

3. Coherent oscillator

For a coherent oscillator, the intensity of the input (signal) wave is a part of the output intensity of the idler wave:

$$I_s(0) = I_i(\ell) R \tag{9}$$

where R is the generalized reflectivity that takes into account all the losses in the feedback loop. By combining equations (9) and (5) we obtain the threshold condition of self-oscillation:

$$(\gamma\ell)_{th} = \sqrt{1/R}. \tag{10}$$

To obtain an oscillation in a lossless cavity ($R = 1$) it is necessary to ensure $(\gamma\ell) \geqslant (\gamma\ell)_{th} = 1$.

With the boundary condition given by equation (9) we obtain from equation (3) the intensity of the oscillation wave as a function of the coupling strength $\gamma\ell$:

$$I_i(\ell) = [I_p(0)/2R]\left[(\gamma\ell)\sqrt{(\gamma\ell)^2 + 4(1+R)} - (\gamma\ell)^2 - 2\right]. \tag{11}$$

One can see that for $R = 1$ the oscillation starts with zero intensity at $\gamma\ell = 1$ and that the oscillation intensity saturates

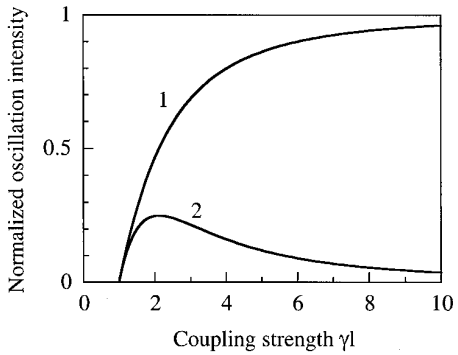

Figure 2. Calculated coupling strength $\gamma\ell$ dependences of the idler wave (1) and signal wave (2) for the coherent oscillator with $R = 1$.

at $I_p(0)$ for large $\gamma\ell$ (figure 2). It should be noted, however, that for $R = 1$ the oscillation wave does not leave the cavity in the direction of the idler wave. At the same time, after one round trip in the feedback loop it is released in part from the cavity as a signal wave s. The output intensity of the signal wave can be calculated from equations (7), (9) and (11):

$$\frac{I_s(\ell)}{I_p(0)} = \left[\frac{I_i(\ell)}{I_p(0)} - \left(\frac{I_i(\ell)}{I_p(0)}\right)^2\right] R. \qquad (12)$$

Curve 2 in figure 2 represents the coupling strength dependence of $I_s(\ell)$. The intensity $I_s(\ell)$ increases at first with $\gamma\ell$ and then reaches a maximum and starts to decrease. This depletion for large $\gamma\ell$ values is related to the intensity growth of the additional wave, $I_a(\ell)$; this wave can also be used as an output wave of the oscillator.

4. Experiment

The schematic representation of the experimental arrangement is shown in figure 3(*a*). A nominally undoped sample of $BaTiO_3$ (measuring $3.6 \times 6.1 \times 6.0$ mm^3 with the optical axis normal to the interaction plane) is exposed to the pump wave p and the signal wave s making an angle $2\theta \approx 12^\circ$. The phase matching condition (equation (1)) imposes a rather narrow acceptance angle window for the signal wave, of the order of a few minutes of arc (roughly defined by the angular selectivity of the recorded grating). This is why a fine adjustment is needed, which is performed by a crystal rotation by a small angle to maximize the steady-state intensity of the idler wave. An unexpanded light beam from an Ar^+ laser (0.515 μm, single mode, single frequency) is divided into two parts to form the signal and pump waves. By introducing the feedback as shown in figure 3(*b*) this amplifier can be transformed into a coherent oscillator.

With the experimental arrangement described above (figure 3(*a*)), we study the conversion of the signal wave into the idler wave with amplification. The intensity of the idler wave gradually increases until the saturation value is reached (figure 4). By decreasing the intensity of the signal wave with an additional phase retarder and a polarizer (not shown in figure 3(*a*)) we check at first that the saturated intensity of the idler wave linearly depends on the input intensity.

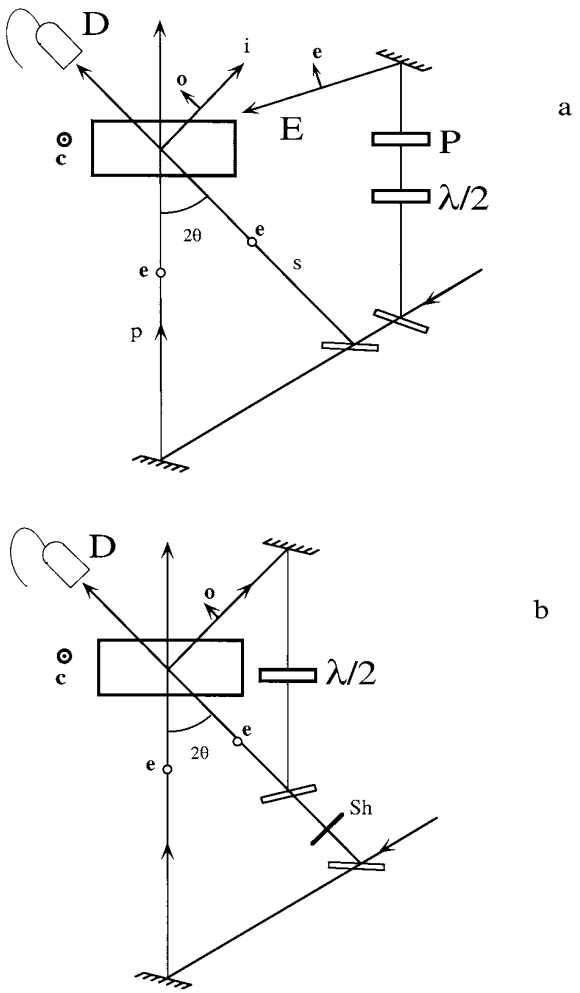

Figure 3. Schematic representation of the experimental arrangement to study the amplification (*a*) and the coherent oscillation (*b*). PRC is a photorefractive crystal, M is a mirror, BS is a beam-splitter, $\lambda/2$ is a half-wave plate, P is a polarizer, Sh is a shutter, D is a photodetector and E is the erasing beam; o and e denote ordinary and extraordinary polarizations of the light waves.

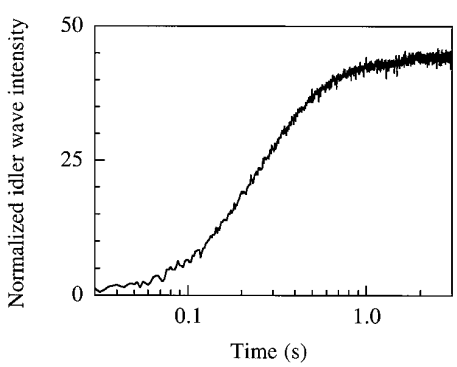

Figure 4. Measurement of the temporal dynamics for the idler wave. The output intensity of the idler wave is normalized to the intensity of the signal wave transmitted through the sample with no pump beam.

An additional erasing light beam that is ordinarily polarized is sent to the sample (beam E in figure 3(*a*)). By changing its intensity with the half-wave plate and the polarizer

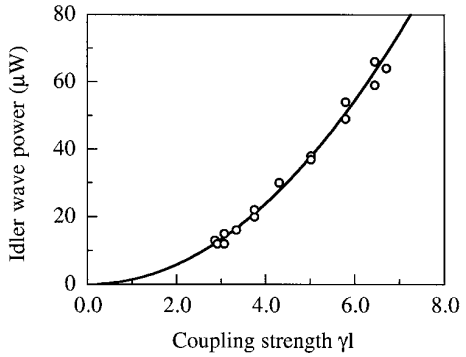

Figure 5. Coupling strength $\gamma\ell$ dependence of the idler wave intensity for $I_s/I_p \approx 10^{-4}$. The open circles represent the experimental values while the solid curve shows the best fit to a power-two dependence.

(see figure 3(*a*)) the coupling strength $\gamma\ell$ is controlled since

$$\gamma\ell = \frac{(\gamma\ell)_o}{[I_{er}\alpha_o \cos^2(2\beta)/I_o\alpha_e] + 1}, \tag{13}$$

where $(\gamma\ell)_o$ is the coupling strength with no erasing beam, I_{er} is the initial intensity of the erasing beam and β is the phase retarder angle with respect to the sample C-axis direction. The absorption coefficients $\alpha_{o,e}$ for different light polarization appear in equation (13) to take into account the difference in photoconductivity for an ordinary or an extraordinary wave. Figure 5 shows the dependence of the idler wave intensity on the coupling strength $\gamma\ell$. The solid curve represents the fit to the power-two dependence.

Two mirrors are used to build a feedback loop for the coherent oscillator (figure 3(*b*)). A fraction of the intensity of the idler wave is reflected by these mirrors back to the input face of the sample in the direction of the signal wave. As the idler wave is an ordinary wave and the signal wave should be an extraordinary one, a phase retarder (half-wave plate) is put inside the feedback loop. A shutter Sh cuts the signal wave, which is used only for cavity adjustment. Like several other configurations of photorefractive oscillators (semilinear, ring loop, two interaction regions [9]) this one has an unclosed cavity: the oscillation wave is leaving the cavity after one round trip but together with the pump wave it maintains a certain constant diffraction efficiency of the photorefractive grating. The anisotropic diffraction of the pump wave from this grating permanently supplies new photons to the oscillation wave.

The dynamics of the oscillation wave intensity is shown in figure 6. The striking difference in the temporal behaviour of the amplified wave (figure 4) and of the oscillation wave is evident: the intensity of the idler wave increases gradually from the very beginning of the exposure and then saturates while the onset of the oscillation is obviously delayed by a certain time called t_{os}. No regular time variation in saturated oscillation intensity is observed; this proves the absence of a frequency shift of the oscillation wave with respect to the pump wave. Random fluctuations of the output intensity may be caused by technical factors (such as insufficient mechanical stability or air convection). It might be expected that, because of its adaptive nature, this oscillator with a phase conjugate

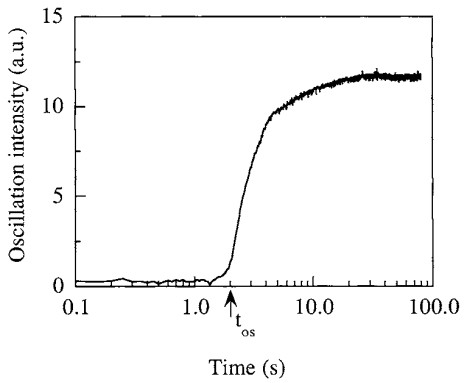

Figure 6. Measured dynamics of the oscillation wave.

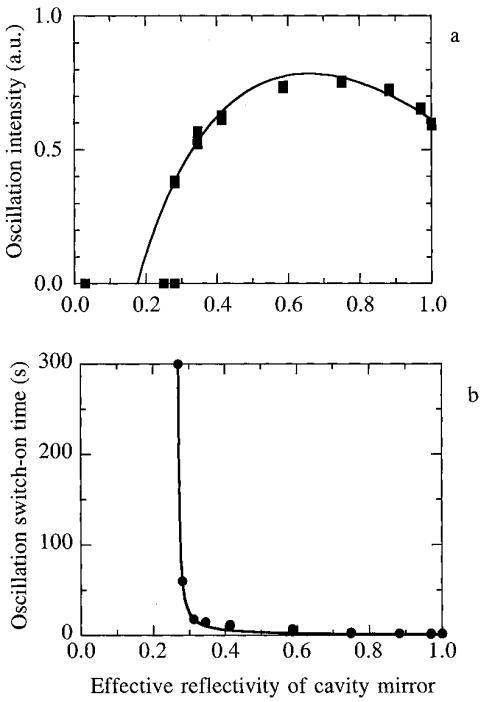

Figure 7. Oscillation intensity (*a*) and oscillation switch-on time (*b*) versus effective reflectivity. The symbols give the measured values and the solid curves show the theoretical fit.

element inside the cavity should be less sensitive to arbitrary phase distortions. This is true however only for relatively slow phase variations with a characteristic time exceeding that of the photorefractive response time.

Furthermore we measure the dependence of the saturated oscillation intensity and oscillation switch-on time t_{os} on cavity losses (figure 7). The losses are introduced by a rotation of the phase retarder in the feedback loop to a certain angle β. This rotation decreases the intensity of the feedback component with the necessary polarization (ordinary wave), i.e. it is equivalent to the decrease of the cavity mirror reflectivity as

$$R_{eff} = R_o \cos^2(2\beta) \tag{14}$$

where R_o stands for the equivalent initial cavity mirror reflectivity.

Figure 7(*a*) clearly shows that the oscillation exists only for $R_{\rm eff}$ exceeding a well defined threshold value. The output oscillation intensity increases at first with the effective reflectivity $R_{\rm eff}$ but it obviously falls off for large values of $R_{\rm eff}$. The oscillation switch-on time, in contrast, is decreasing with $R_{\rm eff}$; it goes to infinity exactly at the threshold (see figure 7(*b*)).

5. Discussion

Let us now compare the experimental results with the calculated ones. For a small input signal ($I_{\rm s} \approx 10^{-4} I_{\rm p}$) the intensity $I_{\rm i}$ of the idler wave generated in this interaction increases proportionally to the input intensity $I_{\rm s}$, in agreement with equation (5). It is amplified as the second power of the coupling strength (figure 5), also in agreement with equation (5). The ultimate amplification $I_{\rm i}(\ell)/I_{\rm s}(0)$ close to 50 leads to an evaluation of the ultimate coupling strength: $\gamma\ell \approx 7$. This value is only 25% smaller than the theoretical estimate deduced from equation (4), with $r_{51} = 1200$ pm V^{-1}, $n \approx 2.5$, $\lambda = 0.515$ μm and at the ambient temperature. The small difference stems from the fact that the space-charge screening is not taken into account in the theoretical expression given by equation (4).

With the value $\gamma\ell \approx 7$ one can expect to obtain the self-oscillation in the cavity shown in figure 3(*b*) for a mirror reflectivity as small as $R = (1/\gamma^2\ell^2) \approx 0.02$. In fact the threshold reflectivity of the cavity mirror is much larger, $R \approx 0.24$ (see figure 7). This is explained, in part, by other losses such as the Fresnel reflections from the sample faces, the linear absorption of the crystal, the imperfect reflectivity of the feedback loop mirrors and the diffraction losses, but the most important contribution to the losses originates from the high angular selectivity of the background parametric process.

Equations (11) and (12) give the output oscillation intensity as a function of the cavity mirror reflectivity R. It should be underlined, however, that the way the losses are introduced in our experiment differs from the simple use of the semi-transparent mirrors to form a cavity. The half-wave plate does reduce the feedback as described by equation (14) but in the zeroth approximation it does not change the total fluence in the sample, $I_{\rm o} = I_{\rm p}(0) + I_{\rm i}(\ell)$ (we neglect the small difference in the absorption coefficients for ordinary wave and extraordinary wave here). Keeping this in mind we obtain from equations (11) and (12) the oscillation intensity:

$$\frac{I_{\rm i}(\ell)}{I_{\rm p}(0)} = -\frac{1}{R} - \frac{(\gamma\ell)^2}{2R} + \sqrt{(\gamma\ell)^4 + 4(\gamma\ell)^2/(1+R)}, \quad (15)$$

$$\frac{I_{\rm s}(\ell)}{I_{\rm p}(0)} = \frac{I_{\rm i}(\ell)}{I_{\rm p}(0)} - \left[\frac{I_{\rm i}(\ell)}{I_{\rm p}(0)}\right]^2 R. \quad (16)$$

The first term in equation (16) does not contain R because both the extraordinary wave with intensity proportional to R, and the ordinary wave with intensity proportional to $(1 - R)$, are transmitted in the same direction, that gives in total a term independent of R. The second term keeps R because only an extraordinary component of the incident signal wave (with intensity proportional to R) is diffracted from the grating; the ordinary component in the incident signal wave is not Bragg matched to the grating.

Note that the squared coupling strength and the reflectivity enter equations (15) and (16) only as a product; this results in a self-similarity of the dependences $I_{\rm i,s}(\ell) = f(R)$ and $I_{\rm i,s}(\ell) = f(\gamma^2\ell^2)$. On the other hand it allows us to renormalize $\gamma^2\ell^2$ in such a way that it is reduced to include all cavity losses except those introduced by a half-wave plate. The solid curve in figure 7(*a*) represents the fit of the experimental data according to equation (16) with $R_{\rm eff}$ given by equation (14). Qualitatively the calculated dependence corresponds quite well to the experimental one except in the vicinity of the threshold, where the measured dependence is more abrupt. The value of the efficient coupling strength (including losses) extracted from this fit is $(\gamma\ell)_{\rm eff} \approx 2.4$, i.e. less than half $\gamma\ell \approx 7$, measured from the idler wave amplification.

The oscillation switch-on time increases dramatically near the threshold of oscillation (figure 7(*b*)). This behaviour is typical for all coherent oscillators and reveals the similarity of the oscillation threshold with a phase transition temperature in solid-state physics [10–12]. The solid curve in figure 7(*b*) represents the data fit to the dependence $1/(R - R_{\rm th})$ with $R_{\rm th}$ standing for the threshold value of the effective mirror reflectivity. The value extracted from the fit, $R_{\rm th} \approx 2.4$, is the same as that measured directly from the dependence of the oscillation intensity versus $R_{\rm eff}$.

To conclude, it has been shown that the parametric mixing with no exponential gain for the signal wave (the real part of the coupling constant is identically zero) may provide idler wave amplification. In spite of the fact that this amplification is less efficient since the process obeys a law $(\gamma\ell)^2$ instead of $\exp(\gamma\ell)$, it can be used successfully to build up different coherent oscillators.

While a power law amplification is rather unusual for photorefractive crystals with nonlocal nonlinear response (index grating $\pi/2$-shifted with respect to the light fringes) it seems to be standard for frequency-degenerate nonlinear interactions in media with local response, for example in $\chi^{(3)}$-media. One can easily find descriptions of numerous experiments on backward-wave four-wave mixing in different $\chi^{(3)}$-materials where the intensity of the phase conjugate wave is measured to increase as $\tan^2(\gamma\ell)$, i.e. $(\gamma\ell)^2$ for small-signal amplification. Papers reporting on coherent oscillation with $\chi^{(3)}$-media are much less frequent (see for a review, e.g., [13]).

Acknowledgments

This work has been supported in part by the Deutsche Forschungsgemeinschaft (SFB 225). The valuable comments and suggestions of the reviewers are gratefully acknowledged.

References

[1] Huignard J-P and Gunter P 1989 *Photorefractive Materials and Their Applications* vol 1 (Berlin: Springer)
[2] Odoulov S and Sturman B 1987 *Sov. Phys.–JETP* **65** 1134

[3] Sturman B, Odoulov S and Goul'kov M 1996 *Phys. Rep.* **275** N4
[4] Temple D and Warde C 1986 *J. Opt. Soc. Am.* B **3** 337–41
[5] Ewbank M, Yeh P and Feinberg J 1986 *Opt. Commun.* **59** 423
[6] Rupp R A and Drees R W 1986 *Appl. Phys.* B **39** 223
[7] Petrov M P, Stepanov S I and Kamshilin A A 1979 *Opt. Laser Technol.* **79** 149
[8] Kukhtarev N, Kraetzig E, Kuelich H-C and Rupp R A 1984 *Appl. Phys.* B **35** 1721
[9] Cronin-Golomb M, Fischer B, White J and Yariv A 1984 *IEEE J. Quantum Electron.* **22** 12
[10] Goul'kov M, Odoulov S and Trott R 1991 *Ukr. Phys. J.* **36** 1007
[11] Engin D, Orlov S, Segev M, Valley G and Yariv A 1995 *Phys. Rev. Lett.* **74** 1743
[12] Odoulov S, Goul'kov M and Shinkarenko O 1999 *Phys. Rev. Lett.* **83** 3637
[13] Odoulov S, Soskin M and Khyzhnjak A 1998 *Coherent Oscillators with Degenerate Four Wave Mixing* (Chur: Harwood)